Accuracy Improvement in Cyclic Voltammetry Stripping Analysis of Thiourea Concentration in Copper Plating Baths

Seunghoe Choe,[a,*] Myung Jun Kim,[a,] Kwang Hwan Kim,[a,*] Hoe Chul Kim,[a,*] Jae Chun Song,[b] Soo-Kil Kim,[c,z] and Jae Jeong Kim[a,**,z]**

[a]*School of Chemical and Biological Engineering, Institute of Chemical Process, Seoul National University, Gwanak-gu, Seoul 151-744, Korea*
[b]*Hanwha Chemical Corp., Jung-gu, Seoul 100-797, Korea*
[c]*School of Integrative Engineering, Chung-Ang University, Dongjak-gu, Seoul 156-756, Korea*

Cyclic voltammetry stripping (CVS) has been regarded as a powerful tool for monitoring the concentrations of organic additives in plating baths. In this study, the dilution titration (DT) method of CVS was modified to improve the measurement accuracy of thiourea (TU) concentrations in Cu plating baths. The conventional DT-CVS method cannot guarantee high accuracy because the electrochemical behavior of TU is concentration and potential dependent, which can cause disturbances in the response signals. In this study, by adding polyethylene glycol (PEG) as an organic additive, the undesirable electrochemical behavior of TU was suppressed and the accuracy of DT-CVS was greatly improved. Using the improved method, the concentrations of TU and its derivatives in the plating bath were measured. The errors between the real and measured concentrations were reduced from 15.0%, 36.0%, and 15.0% using the conventional DT-CVS method to within 3.00%, 6.00%, and 6.00% for TU, N-ethyl thiourea, and N′,N-diethyl thiourea, respectively, using the improved method.
© The Author(s) 2015. Published by ECS. This is an open access article distributed under the terms of the Creative Commons Attribution Non-Commercial No Derivatives 4.0 License (CC BY-NC-ND, http://creativecommons.org/licenses/by-nc-nd/4.0/), which permits non-commercial reuse, distribution, and reproduction in any medium, provided the original work is not changed in any way and is properly cited. For permission for commercial reuse, please email: oa@electrochem.org. [DOI: 10.1149/2.0051506jes]
All rights reserved.

Manuscript submitted January 9, 2015; revised manuscript received February 9, 2015. Published February 14, 2015.

Organic additives are important constituents of the electroplating baths owing to their ability to control the morphology and the film properties of the plated material.[1–17] The organic additives are typically grouped into suppressors, accelerators, and levelers, based on their roles and functionality.[1–17] Examples of organic additives in electroplating baths include bis(3-sulfopropyl) disulfide, polyethylene glycol (PEG), janus green b (JGB), polyethylene imine (PEI), 1,2,3-benzotriazole (BTA), and thiourea (TU).[1,2,6–13,18–29]

TU is a common additive in Cu and Ag electrodeposition baths and induces leveling and grain refining properties.[18–26] TU has been used as an additive either solely or in combination with Cl^- (TU-Cl^-) in baths used for electrodeposition processes involving various current/potential waveforms such as direct current, pulse-, or pulse-reverse waveforms.[20,21,23,24] Various applications of TU as an additive have been studied, including the formation of the Cu twin, Ag superfilling, and the fabrication of CuS nanowire structures.[18,19,23–26]

TU is known to form thiolate complexes such as $[Cu\text{-}(TU)]^{2+}$, $[Cu\text{-}TU]^{+}$, and $[Cu\text{-}(TU)_2]^{2+}$ with Cu^{2+} ions in acidic Cu plating solutions.[20–29] Additionally, TU can be oxidized to formamidine disulfide (FDS), which forms other thiolate complexes with Cu^+ and Cu^{2+} ions.[27–29] Owing to the various derivatives and their different electrochemical responses, TU shows unique electrochemical behavior unlike typical suppressors or levelers. Although TU commonly reduces the Cu deposition rate, it often acts in an opposite role as an accelerator under specific conditions such as low concentrations and low overpotentials.[27–29] Several mechanisms explaining the accelerating effect of TU have been proposed.[27–29]

Generally, the reduction of Cu^{2+} occurs in two steps, namely the reduction of Cu^{2+} to Cu^+, followed by the reduction of Cu^+ to Cu^0. The first step has been known to be the rate-determining step. In the presence of TU, however, additional reactions occur, as described in Eq. 1.[27–29]

$$2Cu^{2+} + 2TU \leftrightarrow 2Cu^{+} + FDS + 2H^{+} \quad [1]$$

Kim et al. reported the accelerating effect of derivatized TU on Cu electrodes.[27] Wang et al. observed the acceleration effect of TU at low concentrations (below 5 ppm), and explained it based on the relatively higher concentration of $[Cu\text{-}FDS]^+$ compared to $[Cu\text{-}TU]^+$ on the Cu surface.[28] Suarez et al. also suggested that the predominance of $[Cu\text{-}FDS]^+$ over $[Cu\text{-}(TU)]^+$ and $[Cu\text{-}(TU)]^{2+}$ at low overpotentials/low concentrations caused the accelerating effect.[29] They explained that the chain reaction involving the reaction described by Eq. 1, the reduction of Cu^+ to Cu^0, and the reduction of FDS to TU was stimulated at low overpotentials/low concentrations.[29]

During electrolysis, the concentrations of the organic additives gradually decrease due to the physical incorporation of the additives in the Cu deposit and chemical/electrochemical decomposition reactions.[30–44] Since the properties of the plated films strongly depend on the concentrations of the organic additives, the performance of the plating solution gradually degrades upon continued use of the plating solution.

For this reason, systems to monitor and control the concentration of the additives have to be installed. Various methods have been developed for monitoring the additive concentrations, including electrochemical techniques such as cyclic voltammetry stripping (CVS) and cyclic pulse voltammetry stripping (CPVS),[31,45–47] and spectroscopic methods such as nuclear magnetic resonance (NMR),[30–33] UV-visible spectroscopy,[34,35] mass spectroscopy,[36–38] and chromatography.[39,40] Among these, CVS and CPVS have been regarded as the most powerful tools because of their simplicity and sensitivity. However, disadvantages of these methods such as the inability to quantify the concentrations of the decomposition by-products and the electrochemically-inactive compounds, have been pointed out.[31] Moreover, the electrochemical responses of the by-products interfere with the CVS signal of the original components, causing a discrepancy between the real and measured values.[31] On the other hand, while spectroscopic methods provide detailed information about the by-products and the electrochemically-inactive compounds in the plating bath, they sometimes require additional pretreatments, which are often time consuming and costly.[30–33,39,40]

In the case of CVS, several analysis techniques such as dilution titration (DT), modified linear approximation technique (MLAT), and response curves (RC) are applied to determine the suppressor, accelerator, and leveler concentrations, respectively.[47,48] In DT-CVS, the suppressor concentration in the target plating solution is determined by the following procedures, namely (1) measurement of the stripping charge (Q_{base}) by CVS of an additive-free plating solution, named as base solution, (2) addition of a small amount of the target plating

*Electrochemical Society Student Member.
**Electrochemical Society Active Member.
zE-mail: jjkimm@snu.ac.kr; sookilkim@cau.ac.kr

Downloaded on 2019-09-02 to IP 49.247.202.102 address. Redistribution subject to ECS terms of use (see ecsdl.org/site/terms_use) unless CC License in place (see abstract).

solution into the base solution, (3) measurement of the normalized stripping charge (Q/Q_{base}) by CVS of the mixture, (4) repetition of procedures (2)-(3) until Q/Q_{base} reaches an end point, referred to as the evaluation ratio which is a predetermined value for titration calculation, and (5) measurement of the volume of the target plating solution at the specific evaluation ratio. Above procedures are identically applied to the standard solution, in which the concentration of suppressor is tightly controlled to make the standard curve (calibration curve) of Q/Q_{base} as a function of suppressor concentration. By comparing the volume of the target solution with that of a standard solution at the evaluation ratio, the suppressor concentration of the target solution can be determined, from the basic titration formula shown in Eq. 2[49]–4.[50]

$$C = C' \text{ [at evaluation ratio]} \quad [2]$$

$$C = C' = \frac{V_p C_p}{V_{base} + V_p} = \frac{V_S C_S}{V_{base} + V_S} \quad [3]$$

$$C_P = \frac{V_S C_S}{V_{base} + V_S} \frac{V_{base} + V_p}{V_P} \quad [4]$$

In the above equation, C is the concentration of suppressor in (target + base) mixture, C′ is the concentration of suppressor in (standard + base) mixture, V_{base} is the volume of the base solution, V_s is the volume of the standard solution at the evaluation ratio, V_p is the volume of the target solution at the evaluation ratio, C_s is the concentration of the suppressor in the standard solution, and C_p is the concentration of the suppressor in the target solution.

Monitoring tools to determine TU concentrations in aqueous medium have been extensively studies elsewhere in purpose of application to the environmental and industrial issues.[51–53] One of the approaches included the electrochemical method based on the redox reactions between TU and FDS.[51] However, the application of electrochemical methods on the quantification of TU in Cu plating solution have been rarely reported in spite of focused researches on the behavior of TU.[18–29] The scarcity of literature on electrochemical monitoring methods for TU in particular is probably due to the unique electrochemical behavior of TU, resulting from its various reduced species and their different electrochemical responses depending on the TU concentration and the applied potential. Owing to the interference from the reduced species, it appears that conventional DT-CVS is unsuitable as a monitoring tool for determining the TU concentrations. Therefore, in this study, DT-CVS was modified to improve the accuracy of the measured TU concentrations in Cu plating baths by adding PEG into the base solution, in order to suppress the undesired electrochemical behavior of TU and its reduced species.

Experimental

Figure 1 shows the experimental set-up used in this study. Cu plating solutions consisting of 0.25 M $CuSO_4$, 1.0 M H_2SO_4, and 0∼1.5 mM TU were used for the CVS and UV-visible spectroscopy experiments. UV-visible spectroscopic measurements (Thermo, Genesys-10) were carried out using deionized water as a blank solution.

CVS (Metrohm, 797A Computrace) was carried out in order to observe the electrochemical response of TU and to measure the normalized stripping charge (Q/Q_{base}). The standard Cu plating solution containing 0.25 M $CuSO_4$, 1.0 M H_2SO_4, and 1.4 mM TU was periodically added to the base solution. The volume of the base solution was 50 mL and the standard solution was periodically added in doses of 0.05 mL. CVS was carried out after each addition, to obtain the stripping charges, which were normalized as (Q/Q_{base}), where Q_{base} was the stripping charge of the base solution. As shown in Figure 1, two types of base solutions were used in the CVS analyses. The conventional base solution, referred to as base solution 1 (BS1) was composed of 0.25 M $CuSO_4$, 1.0 M H_2SO_4, and 1.0 mM NaCl, whereas the modified base solution (BS2) was composed of 0.25 M $CuSO_4$, 1.0 M H_2SO_4, 1.0 mM NaCl, and 90 μM PEG with a molecular weight of 3400.

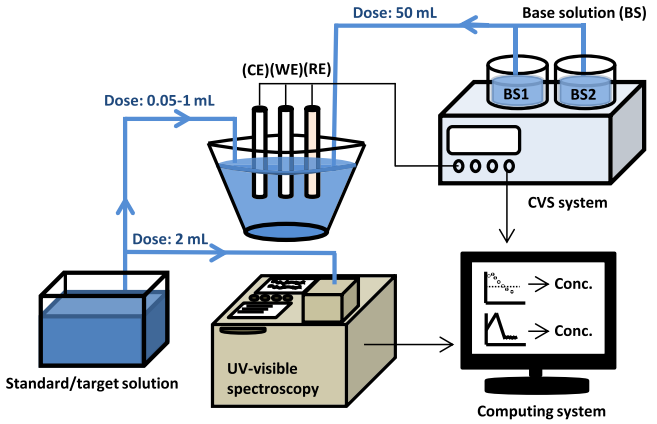

Figure 1. Schematic diagram of the experimental setup.

The electrochemical cell for CVS was composed of a Pt rotating disk electrode (RDE) with an active area of 3.14 mm^2, which acted as the cathode, a Pt rod anode, and an Ag/AgCl [sat. KCl] reference electrode. The rotation speed of the Pt RDE during CVS was fixed at 2000 rpm, which is aimed to support mass transport of TU to the electrode surface, thereby enhancing the inhibiting ability of TU.[54] The voltammograms were obtained with a potential range from 1.575 V to the cathodic vertex potential (−0.1 V∼−0.4 V) with a scan rate of 0.1 V/s.

The influence of the molecular weight of PEG on the CVS results was also studied. A small volume of the standard solution (0.05 mL) containing 0.25 M $CuSO_4$, 1.0 M H_2SO_4, and 1.4 mM TU was periodically added to BS2 solutions (50 mL) containing PEG with molecular weights of 1050 Da, 1500 Da, 3400 Da, and 8000 Da. CVS was carried out after every addition and the stripping charges were obtained. Cathodic vertex potentials for the analyses were fixed at −0.3 V.

Plots of Q/Q_{base} as a function of TU-derivative concentration were obtained for TU-derivatives such as N-ethyl thiourea (ETU) and N′,N-diethyl thiourea (DETU). Small volumes of the standard solutions (0.05 mL) containing 0.25 M $CuSO_4$, 1.0 M H_2SO_4, and 1.4 mM TU-derivatives were periodically added to either BS1 or BS2 solutions (50 mL). The cathodic vertex potentials for the analyses were fixed at −0.3 V.

The accuracy of DT-CVS was evaluated by comparing the real and measured values of the concentrations of the TU-derivatives. Standard solutions comprising of 0.25 M $CuSO_4$, 1.0 M H_2SO_4, and 1.4 mM TU-derivatives were used to generate the calibration curve. The evaluation ratios were 0.8 and 0.6 for BS1 and BS2, respectively and the cathodic vertex potential for the analyses was fixed at −0.3 V. Using the calibration curve, the concentrations of the TU-derivatives in target solution in the range of 0.7–1.4 mM were measured and compared with the real values.

Results and Discussion

UV-visible spectroscopy was applied for the quantification of TU concentrations in Cu plating solutions. Figure 2a presents the UV-visible spectra of Cu plating solutions containing 0–1.5 mM TU. As shown in Figure 2a, the Cu plating solutions containing TU exhibited peaks at 200–300 nm and 340 nm. The former peak resulted from the Cu^{2+} in the plating solution and appeared to have an abnormal shape, since the absorbance exceeded the upper detection limit, owing to the high concentration of Cu^{2+} in the plating solution. Considering the spectra of the individual components, the peak of pure TU was supposed to be at 235 nm. However, this peak was excluded from the analysis because it was buried under the large peak of Cu^{2+}.

Downloaded on 2019-09-02 to IP 49.247.202.102 address. Redistribution subject to ECS terms of use (see ecsdl.org/site/terms_use) unless CC License in place (see abstract).

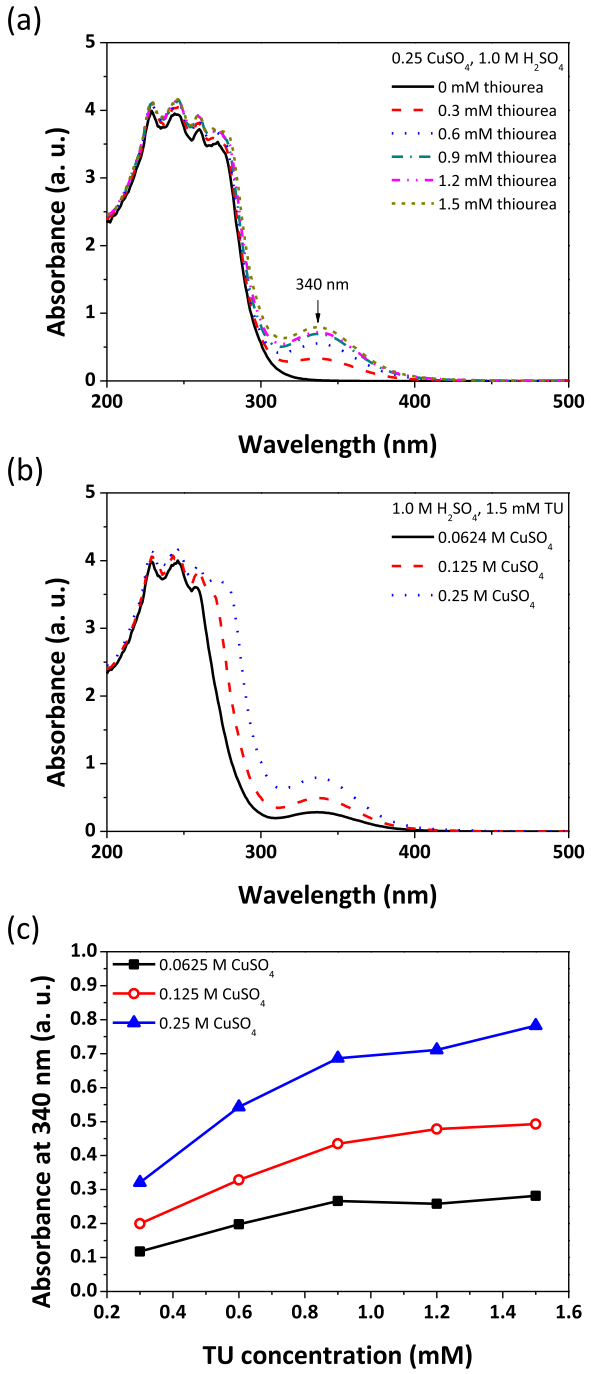

Figure 2. UV-visible spectra of the plating solutions containing various concentrations of (a) TU and (b) $CuSO_4$. The absorbance at 340 nm at various TU concentrations is shown in (c).

Meanwhile, the intensity of the peak at 340 nm initially increased with TU concentration, and subsequently almost converged when the TU concentration was over 0.6 mM. The peak at 340 nm is known to originate from the d-orbital splitting of Cu^{2+}, during the formation of the $[Cu\text{-}(TU)]^{2+}$ complex.[55,56] As shown in Figure 2b, the absorbance increased as the Cu^{2+} concentration increased, confirming that the peak at 340 nm originated from the $[Cu\text{-}(TU)]^{2+}$ complex. The equilibrium among Cu^{2+}, TU, and the $[Cu\text{-}(TU)]^{2+}$ complex is described by Eqs. 5 and 6[55,56]

$$Cu^{2+} + TU \leftrightarrow [Cu - TU]^{2+} \quad [5]$$

$$K = \frac{[Cu - Tu]^{2+}}{[Cu^{2+}][TU]} \quad [6]$$

where K is the equilibrium constant. Figure 2c shows the absorbance at 340 nm as a function of the TU and Cu^{2+} concentrations. As shown in the figure, the absorbance at 340 nm increased with an increase in the concentrations of TU and Cu^{2+}, owing to the equilibrium reaction described in Eq. 5.

When the concentration of Cu^{2+} is significantly higher than that of TU, and the $[Cu\text{-}TU]^{2+}$ is the sole complex formed, the approximate relationship between the absorbance and the concentration of TU can be expressed by Eq. 7.[55]

$$\frac{[TU]_0}{A} = \frac{1}{\varepsilon b K [Cu^{2+}]_0} + \frac{1}{\varepsilon b} \quad [7]$$

Here, A is absorbance, ε is molar absorptivity, b is the cell length, $[Cu^{2+}]_0$ is the bulk concentration of Cu^{2+}, and $[TU]_0$ is the bulk concentration of TU. According to this equation, the absorbance and the concentration of TU are directly proportional to each other. However, as shown in Figure 2c and as reported in the literature,[55] the relationship between the absorbance and the concentration of TU is non-linear, implying that there is a mismatch between the assumption made in arriving at Eq. 7 and the experimental results obtained. A possible explanation for the discrepancy could be the formation of another complex with a higher coordination number such as $[Cu\text{-}(TU)_n]^{2+}$.[55] Based on these results, it appeared that monitoring the TU concentration with UV-visible spectroscopy is effective only in limited concentration ranges.

DT-CVS was also applied for the analysis of TU concentrations in Cu plating solutions. Prior to the application of DT-CVS, the electrochemical responses of TU were studied. Figures 3a–3c present the CVS results in BS1 as the function of TU concentration. As shown in the figures, the addition of TU led to a slight decrease in the current density at all vertex potential values. The inhibition effect was associated with the adsorption of TU on the active sites of the Cu surface. Due to the inhibition effect of TU, the normalized stripping charge (Q/Q_{base}) decreased with TU concentration, as presented in Figure 3d. The figure revealed that the absolute slope of the plot of Q/Q_{base} versus TU concentration decreased as the vertex potential shifted negatively. This tendency appears to be related to the potential-dependent adsorption of TU.[57–61] It is known that the surface coverage of TU decreases as the cathodic overpotential increases because of hydrogen evolution,[57] TU decomposition,[58] and the electrical repulsion force between TU and the substrate.[59] It appears that the low surface coverage of TU at high overpotentials reduces the difference between Q and Q_{base}, resulting in the decrease in the slope of the plot of Q/Q_{base}.

However, as shown in Figure 3d, the value of Q/Q_{base} exceeded 1 at low TU concentrations and less negative vertex potentials, where the acceleration effect dominated the inhibition effect. In addition, Q/Q_{base} decreased non-linearly at less negative vertex potentials (e.g., −0.10 V and −0.15 V). These results revealed the limitations of conventional DT-CVS for the determination of TU concentrations, namely a non-linear Q/Q_{base} drop at less negative vertex potentials and relatively low TU concentrations due to the acceleration effect of TU and a less steep Q/Q_{base} drop at highly negative vertex potentials as a result of the low surface coverage of TU.

It is expected that the elimination of the undesirable accelerating effect may contribute to an improvement in the linearity and the steepness of the Q/Q_{base} drop in the DT-CVS analysis. One possible solution is the addition of PEG to the base solution, since PEG can suppress the accelerating effects by forming a PEG-Cu^{+}-Cl^{-} complex[2,62–64] on the Cu surface. Figures 4a–4d show the CVS results and the corresponding Q/Q_{base} plot in the BS2 solution. As shown in the figures, the current density and the corresponding stripping charge of the base solution (Q_{base}) was significantly reduced in BS2 owing to the inhibition effect induced by the PEG-Cu^{+}-Cl^{-} complex. Meanwhile, as shown in Figure 4d, the use of BS2 resulted in a linear and steep Q/Q_{base} drop even at highly negative vertex potentials. Note that an unusual Q/Q_{base} drop behavior at the vertex potential of −0.2 V might originate from

Downloaded on 2019-09-02 to IP 49.247.202.102 address. Redistribution subject to ECS terms of use (see ecsdl.org/site/terms_use) unless CC License in place (see abstract).

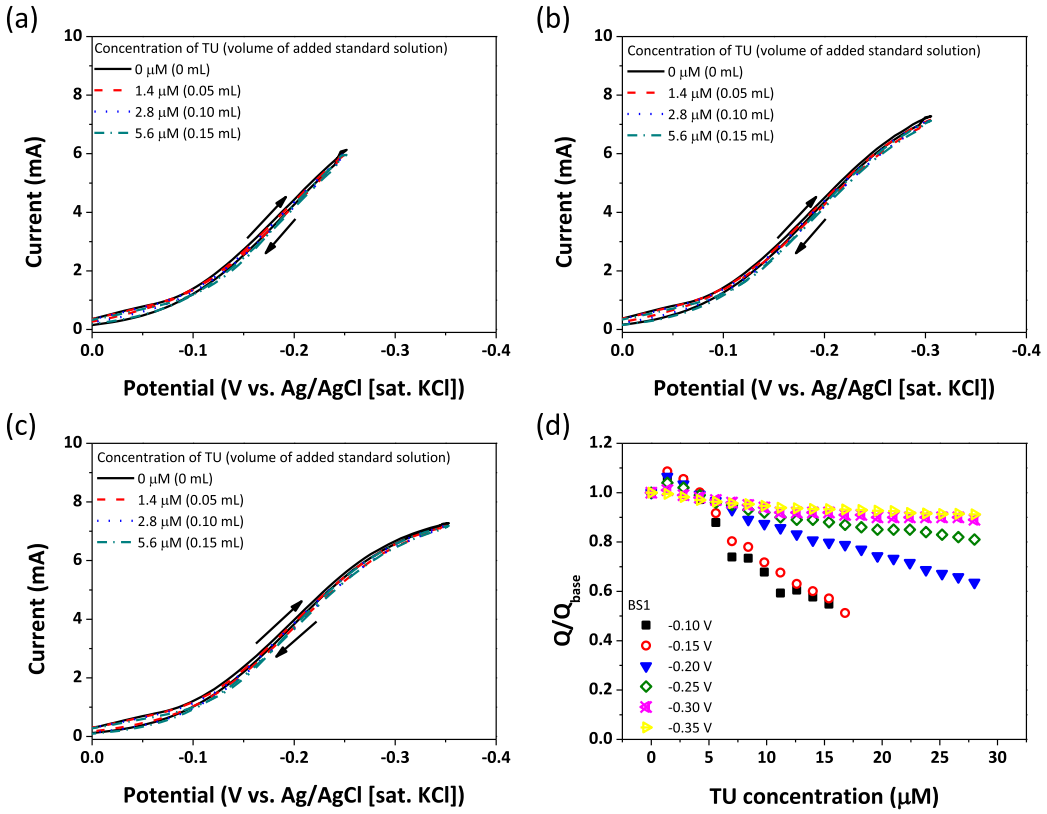

Figure 3. Voltammograms for Cu electrodeposition in BS1 solutions containing various concentrations of TU. (Note that the concentrations of TU are calculated after each additions of standard solutions into 50 mL base solution.) The vertex potentials are (a) −0.25 V, (b) −0.30 V, and (c) −0.35 V. The normalized stripping charges are shown in (d).

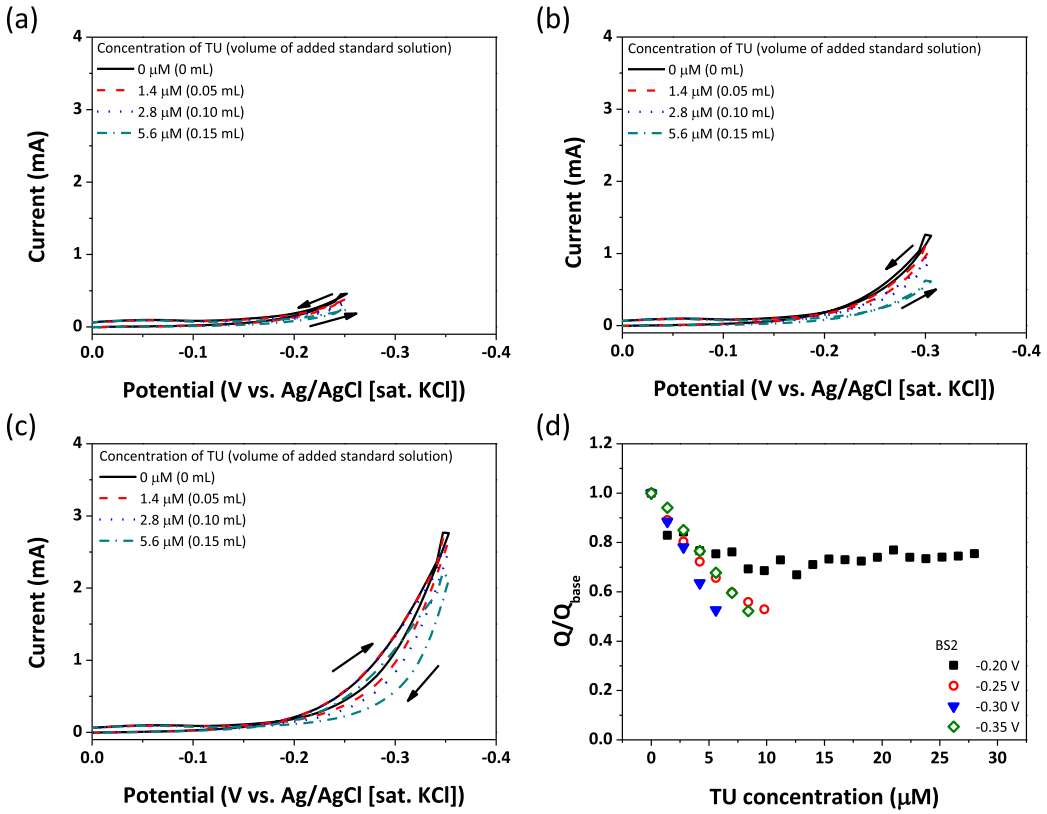

Figure 4. Voltammograms for Cu electrodeposition in BS2 solutions containing various concentrations of TU. (Note that the concentrations of TU are calculated after each additions of standard solutions into 50 mL base solution.) The vertex potentials are (a) −0.25 V, (b) −0.3 V, and (c) −0.35 V. The normalized stripping charges are shown in (d).

Downloaded on 2019-09-02 to IP 49.247.202.102 address. Redistribution subject to ECS terms of use (see ecsdl.org/site/terms_use) unless CC License in place (see abstract).

the saturation of the TU adsorption sites due to the high coverage of PEG. In addition, the acceleration effect from TU clearly disappeared even at low concentrations. Therefore, the linear and steep Q/Q_{base} drop appears to be related to the diminished acceleration effect due to the formation of PEG-Cu^{+}-Cl^{-} on the Cu surface.

Another possibility is the suppression of TU desorption by the added PEG. Unlike the case of BS1, the slopes of the plots of Q/Q_{base} versus TU concentration in the case of BS2 remained high even at very negative vertex potentials (Figure 4d). For confirmation, an additional CVS analysis was carried out with a high concentration of TU, and the results are presented in Figure 5. As shown in Figure 5a, the suppression of Cu plating by TU appears to be effective only in the range of OCP∼−0.2 V. At potentials more negative than −0.2 V, the current densities obtained from BS1+16.8 μM TU became comparable with that from BS1, implying that most of the TU desorbed from the electrodes. Likewise, when the vertex potential was more negative than −0.2 V, the current densities obtained from BS1+16.8 μM TU were almost the same with that from BS1 in the reverse scan, generating a hysteresis curve. The hysteresis curve generated by the sole action of the suppressor has been explained based on the delay between the desorption and the re-adsorption of the suppressor on the Cu surface.[62] As shown in Figure 5a, a hysteresis related to the desorption of TU was clearly observed for vertex potentials of −0.2 V and −0.3 V, whereas it was insignificant for a vertex potential of −0.1 V. However, in the case of BS2 (i.e., the solution containing PEG), while the hysteresis was not clear even at the vertex potential of −0.3 V, it became apparent at the vertex potential of −0.4 V, indicating that the desorption of TU was suppressed by PEG. (Figure 5b)

The influence of the molecular weight of PEG in the BS2 solution was studied next. Figures 6a–6e present the CVS results and the

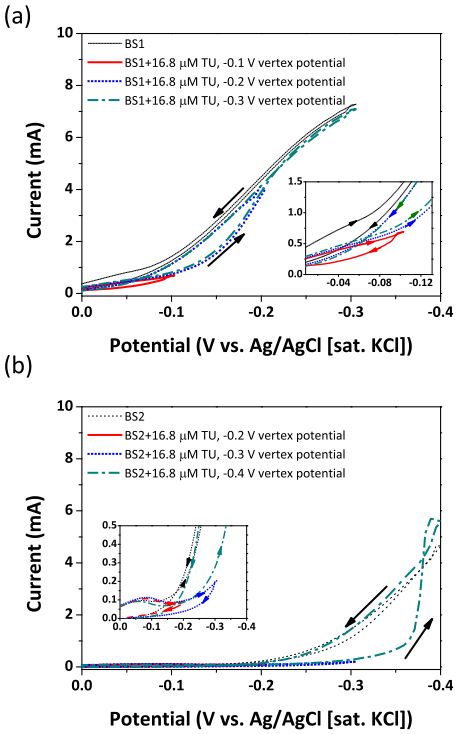

Figure 5. Voltammograms for Cu electrodeposition with various vertex potentials in (a) BS1 and (b) BS2 base solutions.

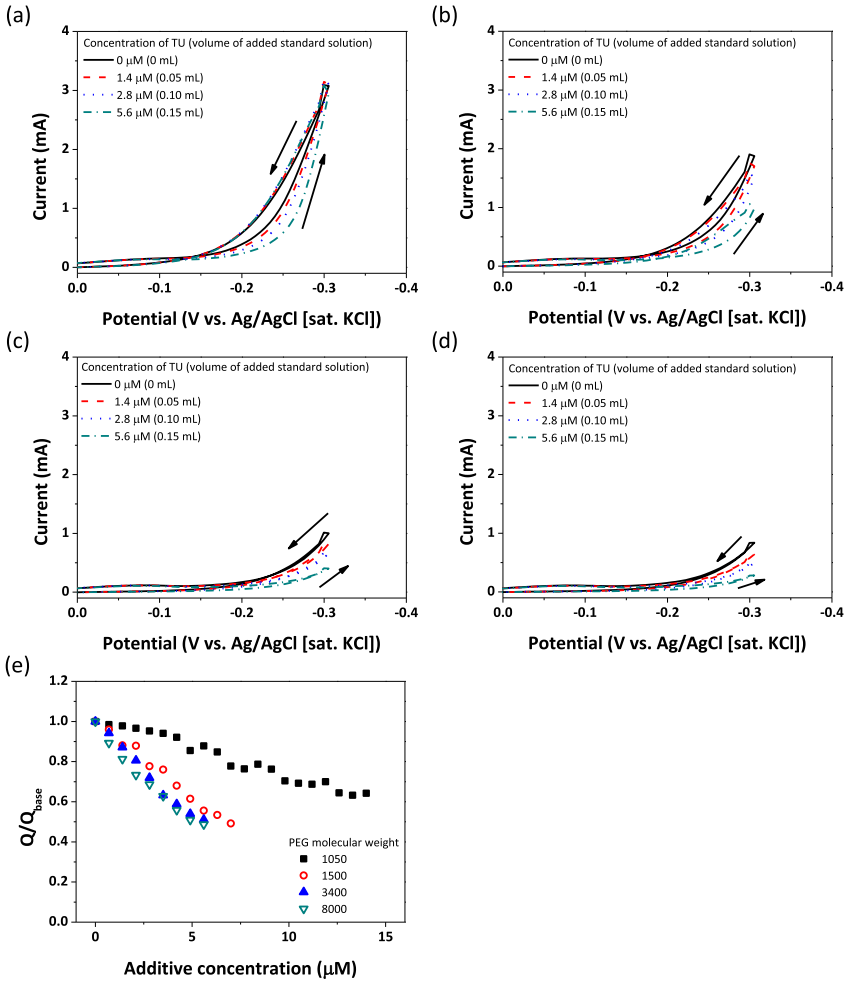

Figure 6. Voltammograms for Cu electrodeposition in BS2 solutions containing PEG with molecular weights of (a) 1050 Da, (b) 1500 Da, (c) 3400 Da, and (d) 8000 Da. (Note that the concentrations of TU are calculated after each additions of standard solutions into 50 mL base solution.) The normalized stripping charges are shown in (e).

Downloaded on 2019-09-02 to IP 49.247.202.102 address. Redistribution subject to ECS terms of use (see ecsdl.org/site/terms_use) unless CC License in place (see abstract).

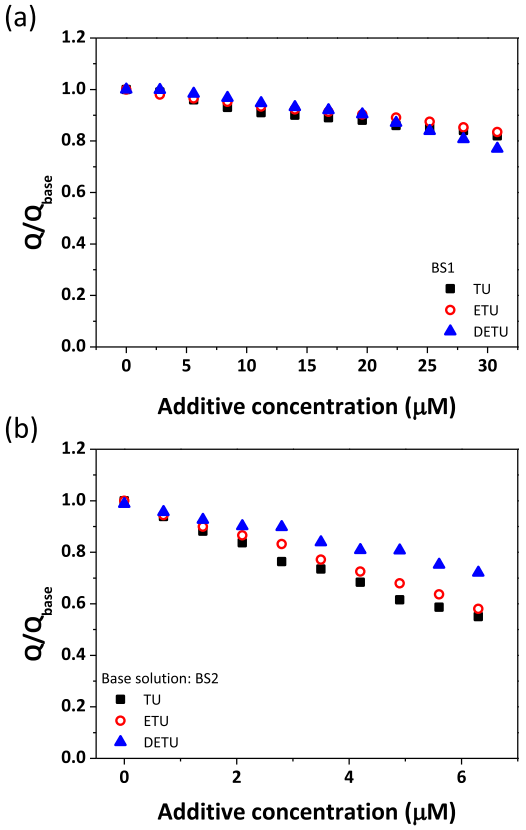

Figure 7. Normalized stripping charges as a function of the concentrations of TU-derivatives in (a) BS1 and (b) BS2 base solutions.

corresponding Q/Q_{base} plot obtained in BS2 solutions containing PEG with various molecular weights. As shown in Figures 6a–6d, the hysteresis curve was clearly seen in the cases of low molecular weight PEG (i.e., for PEG with molecular weights of 1050 Da and 1500 Da), whereas it was insignificant in the case of high molecular weight PEG. This implied that PEG with high molecular weights suppressed either the accelerating effects of TU or the TU desorption itself, more strongly than PEG with low molecular weights. Consequently, the absolute slope of the plot of Q/Q_{base} versus TU concentration increased with the molecular weight of PEG, as seen in Figure 6e. S. Verma et al. reported that TU and PEG could form PEG-embedded TU complex structures.[65] The binding force between TU and PEG could retard the desorption of TU from PEG-covered Cu. Likewise, since the adsorption strength of PEG on the Cu surface increased with molecular weight,[66,67] high-molecular-weight PEG could effectively suppress the desorption of TU.

In order to assess the suitability of this modification for monitoring the concentrations of the derivatives of TU; ETU, and DETU, the Q/Q_{base} plots of TU, ETU, and DETU were obtained using either BS1 or BS2 as the base solutions. Figure 7 revealed that the slope of the Q/Q_{base} plot in the case of BS2 was always higher than that in the case of BS1, regardless of the additives. Meanwhile, the slopes of the Q/Q_{base} plots for the three cases were indistinguishable in the case of BS1, whereas the slopes showed differences according to the number of ethyl groups in the case of BS2. This effect probably came from the steric hindrance of the TU-derivatives during their adsorption on the PEG-covered Cu surface or the difference in the binding force between PEG and the TU-derivatives.

Based on the previous experiments, the concentrations of TU and its derivatives in plating solutions were measured by DT-CVS using either BS1 or BS2 as the base solution. Table I shows the difference between the real and measured concentrations of the TU-derivatives. As shown in Table I, when BS2 was used, the errors between the real and measured concentrations were within 3.00%, 6.00%, and 6.00% for TU, ETU, and DETU, respectively, whereas the errors were originally about 15.0%, 36.0%, and 15.0% for TU, ETU, and DETU when BS1 was used. The improvement in the measurements could be ascribed to the linear and steep Q/Q_{base} drop in BS2 solution. This result demonstrated that the addition of PEG into the base solution enables precise quantification of the concentrations of the TU-derivatives using DT-CVS.

Conclusions

In this study, UV-visible spectroscopy and DT-CVS were applied for the quantification of TU concentrations in acidic Cu plating baths. The results of UV-visible spectroscopy indicated that although a peak related to the $[Cu\text{-}TU]^{2+}$ complex was clearly seen at 340 nm, the peak intensity non-linearly increased with TU concentrations because of the formation of another complex with a higher coordination number. The conventional DT-CVS cannot guarantee high accuracy because the electrochemical behavior of TU is concentration- and potential-dependent, which can cause disturbances in the response signals. In order to resolve this problem, a modified base solution containing PEG was used for the DT-CVS analysis, which led to a steep and stable drop in Q/Q_{base} per unit concentration of TU, ETU, and DETU. The distinguishable and stable Q/Q_{base} drop with the modified base solution was due to the elimination of the undesirable electrochemical behaviors of the TU-related species, by the addition of PEG. With this modified method, we have demonstrated an improvement in the accuracy of DT-CVS in determining the concentrations of TU-derivatives.

Acknowledgment

This work was supported by the Technology Innovation Program (10043789) funded by the Ministry of Knowledge Economy (MKE, Korea). This research was also supported by a grant from the Korea

Table I. Measured concentrations of (a) TU, (b) ETU, and (c) DETU by DT-CVS in BS1 and BS2 solutions and the corresponding errors between the real and measured values.

TU concentration (mM)	Measured in BS1 (mM)	Error (%)	Measured in BS2 (mM)	Error (%)
0.70	0.62	10.9	0.71	1.43
1.05	0.90	14.2	1.08	2.76
1.40	1.35	3.57	1.40	0.71
ETU concentration (mM)	Measured in BS1 (mM)	Error (%)	Measured in BS2 (mM)	Error (%)
0.70	0.95	35.9	0.74	5.42
1.05	1.14	8.67	1.08	2.57
1.40	1.40	0.21	1.40	0.07
DETU concentration (mM)	Measured in BS1 (mM)	Error (%)	Measured in BS2 (mM)	Error (%)
0.70	0.72	3.43	0.66	5.14
1.05	0.90	14.1	1.03	1.90
1.40	1.26	9.86	1.40	0.36

Downloaded on 2019-09-02 to IP 49.247.202.102 address. Redistribution subject to ECS terms of use (see ecsdl.org/site/terms_use) unless CC License in place (see abstract).

CCS R&D Center (KCRC) funded by the Korea government (Ministry of Science, ICT & Future Planning) (NRF-2013M1A8A1056298).

References

1. T. P. Moffat, D. Wheeler, W. H. Huber, and D. Josell, *Electrochem. Solid-State Lett.*, **4**, C26 (2001).
2. T. P. Moffat, D. Wheeler, and D. Josell, *J. Electrochem. Soc.*, **151**, C262 (2004).
3. D. Josell and T. P. Moffat, *J. Electrochem. Soc.*, **160**, D3009 (2013).
4. Y.-D. Chiu and W.-P. Dow, *J. Electrochem. Soc.*, **160**, D3021 (2013).
5. D. Josell and T. P. Moffat, *J. Electrochem. Soc.*, **160**, D3035 (2013).
6. S.-K. Kim and J. J. Kim, *Electrochem. Solid-State Lett.*, **7**, C101 (2004).
7. S.-K. Kim, S. Hwang, S. K. Cho, and J. J. Kim, *Electrochem. Solid-State Lett.*, **9**, C25 (2006).
8. M. J. Kim, H. C. Kim, S.-H. Kim, S. Yeo, O. J. Kwon, and J. J. Kim, *J. Electrochem. Soc.*, **160**, D3057 (2013).
9. M. J. Kim, T. Lim, K. J. Park, S.-K. Kim, and J. J. Kim, *J. Electrochem. Soc.*, **160**, D3081 (2013).
10. M. J. Kim, T. Lim, K. J. Park, S.-K. Kim, and J. J. Kim, *J. Electrochem. Soc.*, **160**, D3088 (2013).
11. N. T. M. Hai, J. Furrer, F. Stricker, T. M. T. Huynh, I. Gjuroski, N. Luedi, T. Brunner, F. Weiss, A. Fluegel, M. Arnold, I. Chang, D. Mayer, and P. Broekmann, *J. Electrochem. Soc.*, **160**, D3116 (2013).
12. K. H. Kim, T. Lim, S. Choe, I. Choi, S. H. Ahn, M. J. Kim, K. J. Park, M. H. Lee, J. J. Kim, and O. J. Kwon, *J. Electrochem. Soc.*, **160**, D3206 (2013).
13. M. J. Kim, H. C. Kim, S. Choe, J. Y. Cho, D. Lee, I. Jung, W.-S. Cho, and J. J. Kim, *J. Electrochem. Soc.*, **160**, D3221 (2013).
14. M. Takeuchi, Y. Yamada, M. Bunya, S. Okada, N. Okamoto, T. Saito, and K. Kondo, *J. Electrochem. Soc.*, **160**, D3110 (2013).
15. A. J. Joi, R. Akolkar, and U. Landau, *J. Electrochem. Soc.*, **160**, D3001 (2013).
16. T. M. T. Huynh, N. T. M. Hai, and P. Broekmann, *J. Electrochem. Soc.*, **160**, D3063 (2013).
17. D. Wheeler, T. P. Moffat, and D. Josell, *J. Electrochem. Soc.*, **160**, D3260 (2013).
18. M. J. Kim, S. H. Yong, H. S. Ko, T. Lim, K. J. Park, O. J. Kwon, and J. J. Kim, *J. Electrochem. Soc.*, **159**, D656 (2012).
19. M. J. Kim, K. J. Park, T. Lim, O. J. Kwon, and J. J. Kim, *J. Electrochem. Soc.*, **160**, D3126 (2013).
20. N. Tantavichet and M. D. Pritzker, *Electrochimica Acta*, **50**, 1849 (2005).
21. N. S. Tantavichet Damronglerd and M. D. Pritzker, *Electrochimica Acta*, **55**, 240 (2009).
22. M. S. Kang, S.-K. Kim, K. Kim, and J. J. Kim, *Thin Solid Films*, **516**, 3761 (2008).
23. K. Shravan Kumar, Krishanu Biswas, and R. Balasubramaniam, *J. Nanopart. Res*, **13**, 6005 (2011).
24. K. Shravan Kumar and Krishanu Biswas, *Surf. Coat. Technol.*, **214**, 8 (2013).
25. A. Ghahremaninezhad, E. Asselin, and D. G. Dixon, *Electrochem. Commun.*, **13**, 12 (2011).
26. A. Ghahremaninezhad, E. Asselin, and D. G. Dixon, *J. Phys. Chem. C*, **115**, 9320 (2011).
27. H. C. Kim, M. J. Kim, S. Choe, T. Lim, K. J. Park, K. H. Kim, S. H. Ahn, S.-K. Kim, and J. J. Kim, *J. Electrochem. Soc.*, **161**, D749 (2014).
28. C. T. Wang and T. J. O'Keefe, in *Proceedings of the International Symposium on Electrochemistry* (edited by P. E. Richardson, S. Srinivasan, and R. Woods), The Electrochemical Society, Pennington, NJ, 655 (1982).
29. D. F. Suarez and F. A. Olson, *J. Appl. Electrochem.*, **22**, 1002 (1992).
30. S. Choe, M. J. Kim, H. C. Kim, S. K. Cho, S. H. Ahn, S.-K. Kim, and J. J. Kim, *J. Electrochem. Soc.*, **160**, D3179 (2013).
31. S. Choe, M. J. Kim, H. C. Kim, T. Lim, K. J. Park, K. H. Kim, S. H. Ahn, A. Lee, S.-K. Kim, and J. J. Kim, *J. Electroanal. Chem.*, **714–715**, 85 (2014).
32. A. Barriola, J. I. Miranda, M. Ostra, and C. Ubide, *Anal. Bioanal. Chem.*, **398**, 1085 (2010).
33. M. Ostra, C. Ubide, and M. Vidal, *Anal. Bioanal. Chem.*, **399**, 1907 (2011).
34. S.-K. Kim and J. J. Kim, *Electrochem. Solid-State Lett.*, **7**, C98 (2004).
35. A. Barriola, E. Garcia, M. Ostra, and C. Ubide, *J. Electrochem. Soc.*, **155**, D480 (2008).
36. W.-H. Wang, C.-C. Hung, S.-C. Chang, and Y.-L. Wang, *J. Electrochem. Soc.*, **157**, H131 (2010).
37. C.-C. Hung, W.-H. Lee, S.-Y. Hu, S.-C. Chang, K.-W. Chen, and Y.-L. Wang, *J. Vac. Sci. Technol. B*, **26**, 255 (2008).
38. W. Wang, Y.-B. Li, and Y.-L. Li, *Appl. Surf. Sci.*, **255**, 4389 (2009).
39. L. D'Urzo, H. Wang, A. Pa, and C. Zhi, *J. Electrochem. Soc.*, **152**, C243 (2005).
40. L. D'Urzo, H. Wang, C. Tang, A. Pa, and C. Zhi, *J. Electrochem. Soc.*, **152**, C697 (2005).
41. M. Stangl, J. Acker, S. Oswald, M. Uhlemann, T. Gemming, S. Baunack, and K. Wetzig, *Microelectron. J.*, **84**, 54 (2007).
42. M. Stangl, J. Acker, V. Dittel, W. Gruner, V. Hoffmann, and K. Wetzig, *Microelectron. J.* **82**, 189 (2005).
43. G. Fabricius, K. Kontturi, and G. Sundholm, *J. Appl. Electrochem.*, **26**, 1179 (1996).
44. K. Taniguchi, M. Dobashi, H. Sakai, and Y. Hara, US patent, 6652725 (2003).
45. L. T. Koh, G. Z. You, S. Y. Lim, C. Y. Li, and P. D. Foo, *Microelectron. J.* **32**, 973 (2001).
46. L. T. Koh, G. Z. You, C. Y. Li, and P. D. Foo, *Microelectron. J.* **33**, 229 (2002).
47. G. Chalyt, P. Bratin, M. Pavlov, A. Kogan, and M. J. Perpich, U.S. Pat. 6572753 (2003).
48. Z.-W. Sun, C. Yu, B. Metzger, D. W. Nguyen, and G. Dixit, U.S. Patent 6808611 (2004).
49. G. Gran, *Analyst*, **77**, 661 (1952).
50. Dongseo linetech, Analysis of organic additive and metal ion using voltammetric method.
51. N. Spataru, T. Spataru, and A. Fujishima, *Electroanal.*, **17**, 800 (2005).
52. J. Rethmeier, G. Neumann, C. Stumpf, A. Rabenstein, and C. Vogt, *J. Chromatogr.*, **934**, 129 (2001).
53. H. J. Bowley, E. A. Crathorne, and D. L. Gerrard, *Analyst*, **111**, 539 (1986).
54. S. S. Kruglikov, N. T. Kudriavtsev, G. F. Vorobiova, and A. Y. Antonov, *Electrochimica Acta*, **10**, 253 (1965).
55. C. J. Doona and D. M. Stanbury, *Inorg. Chem.*, **35**, 3210 (1996).
56. C. J. Doona and D. M. Stanbury, *J. Phys. Chem.*, **98**, 12630 (1994).
57. G. Horanyi and E. M. Rizmayer, *J. Electroanal. Chem.*, **149**, 221 (1983).
58. D. Papapanayiotou, R. N. Nuzzo, and R. C. Alkire, *J. Electrochem. Soc.*, **145**, 3366 (1998).
59. G. Garcia, V. A. Macagno, and G. I. Lacconi, *Electrochimica Acta*, **48**, 1273 (2003).
60. A. Łukomska, S. Smolinski, and J. Sobkowski, *Electrochimica Acta*, **46**, 3111 (2001).
61. J. O'M. Bockris, B. R. Scharifker, and J. L. Carbajal, *Electrochemica Acta*, **31**, 799 (1987).
62. M. E. H. Garrido and M. D. Pritzker, *J. Electrochem. Soc.*, **155**, D332 (2008).
63. Z. V. Feng, X. Li, and A. A. Gewirth, *J. Phys. Chem. B*, **107**, 9415 (2003).
64. B. Bozzini, L. D'Urzo, C. Mele, and V. Romanello, *J. Mater. Sci.*, **17**, 915 (2006).
65. S. Verma, S. L. Jain, and B. Sain, *Tetrahedron Lett.*, **51**, 6897 (2010).
66. W.-P. Dow, M.-Y. Yen, W.-B. Lin, and S.-W. Ho, *J. Electrochem. Soc.*, **152**, C769 (2005).
67. S.-L. Ko, J.-Y. Lin, Y.-Y. Wang, and C.-C. Wan, *Thin Solid Films*, **516**, 5046 (2008).

Downloaded on 2019-09-02 to IP 49.247.202.102 address. Redistribution subject to ECS terms of use (see ecsdl.org/site/terms_use) unless CC License in place (see abstract).